EXPERIMENTAL STUDIES ON THE SHEAR CAPACITY OF CONTINUOUS PRESTRESSED CONCRETE BEAMS WITH EXTERNAL PRESTRESSING

Martin Herbrand, Institute of Structural Concrete, RWTH Aachen University, Germany
Josef Hegger, Institute of Structural Concrete, RWTH Aachen University, Germany

ABSTRACT

The majority of the existing bridge structures on the German Federal Highways was built in the 1960s and 1970s as continuous prestressed concrete beams. According to the current German Bridge Design Code, their calculated shear capacity is often insufficient, which is mainly due to the increased traffic loads and changes in the bridge design methods since their construction. In these cases, the shear capacity may be calculated by applying refined design methods or increased by strengthening measures, e.g. additional external tendons.

This paper presents the results of a research project about the influence of additional external prestressing on the shear capacity of continuous prestressed concrete beams that was carried out at the Institute of Structural Concrete at RWTH Aachen University. Since there is a scarcity of tests on continuous beams, six shear tests on three continuous beams with a low amount of shear reinforcement featuring parabolic and additional external tendons were performed. The test results are presented as well as a comparison between the calculated shear capacities according to different approaches. It was determined whether the shear capacity is accurately predicted by the current design codes or if the shear capacity can be calculated more precisely by alternative approaches, especially regarding the influence of additional external tendons.

Keywords: Bridges, Design, Shear, Continuous Beam, Prestressed, Parabolic Tendon, External Tendon

INTRODUCTION

Most of the existing bridges of the German Federal Highways were built during the 1960s and 1970s as prestressed concrete bridges (Fig. 1, left). They were often designed according to the "Traffic Load Model SLW60" of the German code DIN 1072[1], which consists of an overall heavy goods vehicle load of 600 kN (134.9 kip), a uniformly distributed load of 5 kN/m² in the primary lane and 3 kN/m² on the remaining bridge deck area.

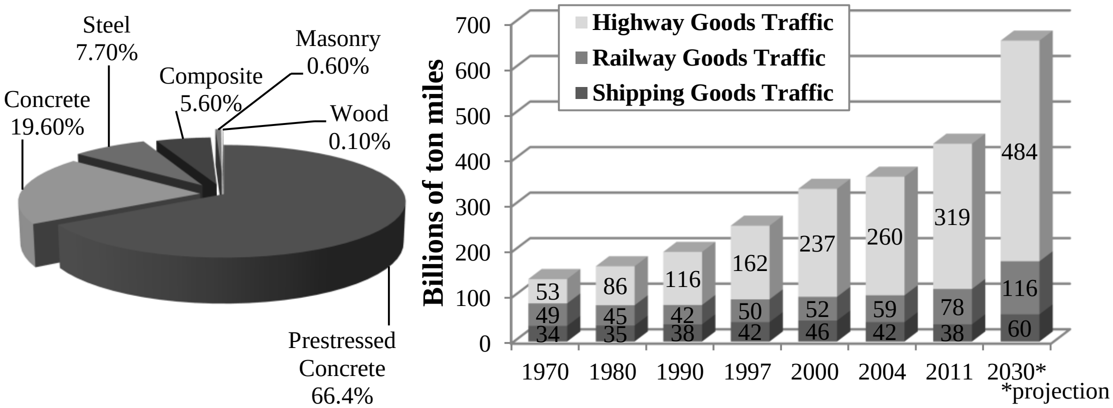

Fig. 1 *left:* Highway Bridges in Germany[2]; *right:* Heavy Goods Traffic in Germany[3]

The shear check was based on the principal tensile strength criterion according to the German code for prestressed concrete DIN 4227[4,5]. In contrast, the shear check according to the current design code for concrete bridges DIN-FB 102[6] is based on the so-called "strut-and-tie model with crack friction,"[7] which is similar to the procedure in EN 1992-2[8]. Since the load model has now been adjusted[9] due to the rising traffic loads (Fig. 1, right) and the new shear check is more conservative, more shear reinforcement is now required in the web as well as a certain amount of minimum shear reinforcement. Therefore, post-strengthening measures are necessary for many bridges in order to extend their service life. One way to strengthen bridges is to apply additional prestressing by external tendons. Within the research project presented in this paper, six shear tests on three continuous beams with and without external prestressing were performed. The aim of the project was to determine the effect of additional external tendons on the shear capacity of continuous prestressed concrete beams, as well as to verify refined methods for calculating the shear capacity of prestressed concrete beams. Therefore, the shear design method of the German bridge design code DIN-FB 102[6], and an alternative approach by Goertz[10] are presented in the following.

SHEAR DESIGN

GERMAN BRIDGE DESIGN CODE DIN-FB 102

In the German bridge design code DIN-FB 102[6] the shear capacity of beams without shear reinforcement (V_{MC90}) is calculated according Eq. (1), which is based on the *fib* Model Code 1990[11].

$$V_{Rd,ct} = \left[c_d \cdot k \cdot \left(100\rho_l \cdot f_{ck}\right)^{1/3} - 0.12\sigma_{cd} \right] \cdot b_w \cdot d \quad (1)$$

where c_d = 0.15 / γ_c (design factor)
γ_c = 1.5 (safety factor)
$k = 1 + \sqrt{200/d} \leq 2.0$ (depth factor)
$\rho_l = A_{sl} / b_w \cdot d$ (longitudinal reinforcement ratio)
A_{sl} Area of the longitudinal tensile reinforcement
b_w smallest width of the cross-section in the tensile zone
d effective depth to tensile reinforcement
f_{ck} characteristic concrete cylinder strength in
σ_{cd} stress on gross cross-section at the center line, compressive stresses are negative

In sections of the beams where the tensile stresses do not exceed the design value of the tensile strength of concrete $f_{ctd} = f_{ctk,0.05}/\gamma_c$, the shear capacity can be calculated according to the shear tension resistance (V_{TC}) (Eq. (2)). The shear capacity calculated by this approach is also the initial shear crack load. For I- and T-shaped beams, the shear capacity has to be determined at different points in the cross-section in order to find the minimum value.

$$V_{Rd,ct} = \frac{I \cdot b_w}{S} \sqrt{\left(\frac{f_{ctk;0.05}}{\gamma_c}\right)^2 - \alpha_l \cdot \sigma_{cd} \cdot \left(\frac{f_{ctk;0.05}}{\gamma_c}\right)} \tag{2}$$

where I second moment of area of the section
S first moment of area of the section at the level considered
$f_{ctk,0.05}$ 5%-fractile of the concrete tensile strength
γ_c = 1.5 (safety factor)
α_l factor to account for the transmission length in prestressed constructions
σ_{cd} stress on gross cross-section at the level considered

The shear capacity of members with vertical shear reinforcement may be calculated according to the truss model (V_{TRUSS}) (Eq. (3)).

$$V_{Rd,sy} = a_{sw} \cdot z \cdot f_{yd} \cdot \cot\theta \tag{3}$$

where $a_{sw} = A_{sw} / s$ (area of shear reinforcement within a distance of s)
A_{sw} area of the vertical shear reinforcement
z inner lever arm between tensile reinforcement and compression chord
s spacing of vertical stirrups
f_{yd} design strength of the shear reinforcement
θ angle of inclination of diagonal compressive stresses

For determining the shear capacity of existing bridges, the angle of inclination $\cot\theta$ may be varied within the limits of Eq. (4)[12].

$$0.57 \leq \cot\theta \leq \frac{1.2 - 1.4\,\sigma_{cd} / f_{cd}}{1 - V_{Rd,c} / V_{Ed}} \leq 3.0 \tag{4}$$

where f_{cd} design value of concrete compressive strength

σ_{cd} stress at the center line of the gross cross-section, compressive stresses are negative

V_{Ed} design shear force in the section considered resulting from external loading and prestressing

In this equation, $V_{Rd,c}$ is the shear force that is transferred by a diagonal crack in the beam (Eq. (5)).

$$V_{Rd,c} = 0.24 \cdot f_{ck}^{1/3} \cdot \left(1 + 1.2 \frac{\sigma_{cd}}{f_{cd}}\right) \cdot b_w \cdot z \tag{5}$$

where f_{ck} characteristic concrete cylinder strength

σ_{cd} stress at the center line of the gross cross-section, compressive stresses are negative

f_{cd} design value of concrete compressive strength

b_w smallest width of the cross-section in the tensile zone

z inner lever arm between tensile reinforcement and compression chord

APPROACH BY GOERTZ

The shear design approach by Goertz is based on the work of Zink, who investigated the shear capacity of prestressed concrete beams without shear reincorcement[13]. In the procedure by Goertz[10], the shear resistance consists of a truss contribution V_s and a concrete contribution V_c (Eq. (6)). The procedure is applicable for members both with and without shear reinforcement.

$$V = V_s + V_c \tag{6}$$

The truss contribution V_s is the minimum value between the capacity of the stirrups and the capacity of the compressive strut (Eq. (7)).

$$V_s = \min \begin{cases} a_{sw} \cdot f_y \cdot z \cdot \cot \beta_r \\ \alpha_c \cdot f_{cm} \cdot b_w \cdot z \big/ \cot \beta_r + \tan \beta_r \end{cases} \tag{7}$$

with f_{cm} mean value of concrete compressive strength

$\alpha_c = 0.75 \cdot \eta_1 = 0.75$ (standard concrete)

The crack angle β_r is calculated by Eq. (8). The equation is based on a linearization of the equation for the compression strut angle according to the shear tension resistance. The effect of stirrups on the crack angle is accounted for by considering the mechanical shear reinforcement ratio $\omega_{w,ct}$.

$$\cot \beta_r = \min \begin{cases} 1 + 0.15 \big/ \omega_{w,ct} - 0.18 \cdot \sigma_x \big/ f_{ctm} \\ 2.15 \\ a/d \end{cases} \tag{8}$$

with $\omega_{w,ct} = (a_{sw}/b_w) \cdot (f_{yk}/f_{ctm})$ (mechanical shear reinforcement ratio)

a_{sw} area of shear reinforcement within a distance of s

b_w smallest width of the cross-section in the tensile zone

f_{yk} characteristic strength of the shear reinforcement

f_{ctm} mean value of concrete tensile strength

σ_x compressive stress on gross cross-section in the center line
a distance between point load and support
d effective depth to tensile reinforcement

The concrete contribution V_c consists of the contributions of the uncracked compression area $V_{c,s}$ and the strut contribution that is favoured by prestressing $V_{c,p}$ (Eq. (9)).

$$V_c = \kappa_s \cdot V_{c,s} + \kappa_p \cdot V_{c,p} \tag{9}$$

with $\kappa_s = 1 - \omega_{w,ct}/3$
$\kappa_p = 1 - \omega_{w,ct}$

The reduction factors κ_s and κ_p account for the influence of the smaller stiffness of the concrete contribution relative to the truss contribution. The equation for the concrete contribution $V_{c,s}$ (Eq. (10)) is based on the work of Zink[13].

$$V_{c,s} = \beta \cdot \frac{2}{3} k_x \, f_{ctm} \, (4d/a)^{0,25} \cdot (5 l_{ch}/d)^{0,25} \cdot b_{s,eff} \cdot d \tag{10}$$

with β $= 3/(a/d) \geq 1{,}0$
l_{ch} $= E_{cm} \cdot G_f / f_{ctm}^2$
G_f $= \min\{0.0307\text{mm} \cdot f_{ctm}; 0.143 \text{ N/mm}\}$ (cracking energy)
f_{ctm} mean value of concrete tensile strength
E_{cm} Young's modulus of concrete
$b_{s,eff}$ $= b_w + 0.6 \cdot h_f$ (effective width of the compressive zone)
h_f height of the flange in compression

The factor k_x represents the height of the concrete compression zone. The factor was modified in this research project to account for the influence of additional external tendons.

$$k_x \approx 0.9 \cdot (\rho_1 \cdot n)^{0.4 - 0.9 \cdot m} \tag{11}$$

with $\rho_1 = A_{s1} / (b_{s,eff} \cdot d)$
A_{s1} Area of the longitudinal reinforcement
$n = E_s / E_c$
E_s Young's modulus of steel
$m = \frac{\sigma_{c,ext}}{f_{cm}} \cdot \frac{A_c}{b_{s,eff} \cdot d}$ (degree of external prestressing)
σ_{cext} compressive stress on cross-sectional area A_c due to external prestressing

In a research project, it was shown that in case of small amounts of shear reinforcement, a direct compression strut exists in prestressed concrete beams[14]. The strut contribution favoured by prestressing $V_{c,p}$ can be calculated according to Eq. (12).

$$V_{c,P} = P \cdot \frac{\Delta z_P}{a} \tag{12}$$

$V_{c,p}$ is the vertical component of the compression strut that is caused by the prestressing force P. In case of prestressed concrete continuous beams, the inner lever arm Δz_P may be taken as the distance between the resulting compressive forces at the load initiation point and the mid support (Fig. 2).

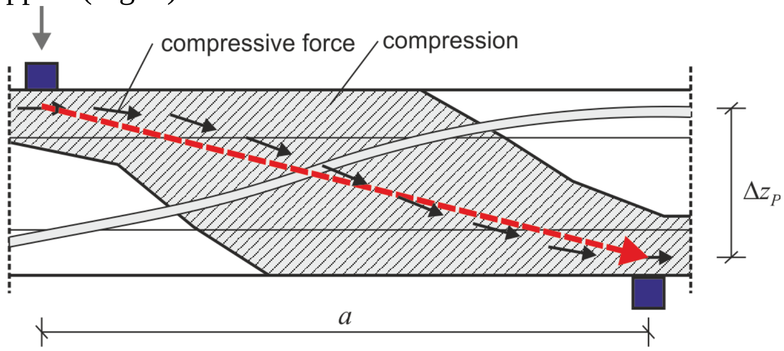

Fig. 2 Compressive forces and direct compression strut at the mid support

EXPERIMENTAL INVESTIGATIONS

TEST SETUP

The test program consisted of six tests on three prestressed two-span beams. The test setup and the loading conditions are shown in Fig. 3. The beams had a total length of 11.3 m (37'0.9") and a cross-sectional height of 0.61 m (24.0"). The load points were located at a distance of a = 2.0 m (6'6.7") from the mid support so that the shear slenderness of the specimen amounted to a/d = 3.6. All of the beams were prestressed seven days after concreting with an internal parabolic tendon consisting of three 0.6" (15.2 mm) strands of prestressing steel St1570/1770 with a cross-sectional area of 3x140 mm² and a prestressing force of P_0 = 430 kN (97 kip).

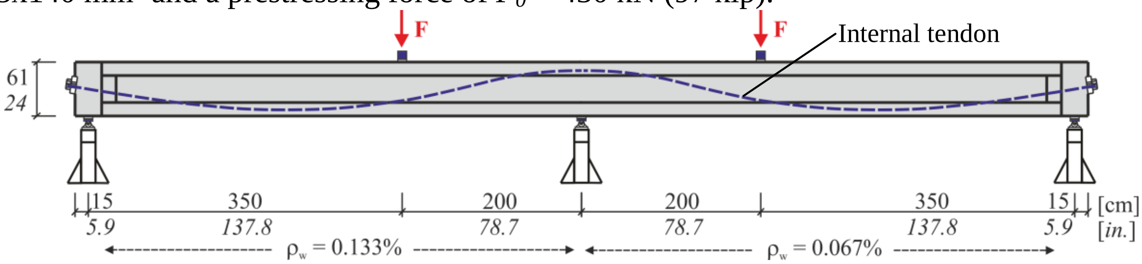

Fig. 3 Test setup and position of the point loads

While the first test beam (TB1) only had an internal tendon, the second and the third beams (TB2 and TB3) had additional external longitudinal prestressing using two sets of three 0.6" (15.2 mm) strands. The additional external tendons were applied one week after the internal prestressing and one week before testing. The shear reinforcement consisted of stirrups (Ø = 6 mm) spaced at 25 cm (9.8") in the left span (ρ_w = 0.133 %), which is about the minimum shear reinforcement required by DIN-FB 102[4], and 50 cm (19.7") in the right span (ρ_w = 0.067 %), which is about half of the minimum shear reinforcement. Shear failure first occured in the right span of the specimen which was subsequently strengthened with tie rods (Fig. 4). A second test was performed in which the left span of the specimen failed.

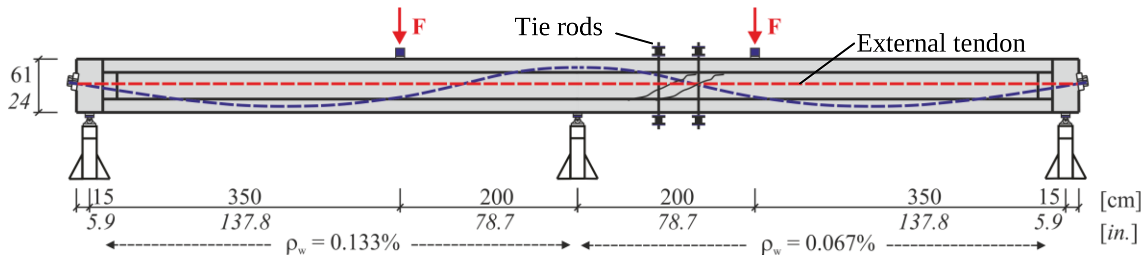

Fig. 4 Test beam with additional external tendons and tie rods

The prestressing forces and material properties are summarized in Table 1. TB2 and TB3 had additional external prestressing forces of 270 kN (60.7 kip) and 450 kN (101.2 kip), respectively. The compressive stresses on the cross-section at the mid support by internal and external prestressing ($\sigma_{c,int}$ and $\sigma_{c,ext}$) already include losses due to friction, creep and shrinkage. The friction coefficients μ of the duct were calculated by measuring the force within the parabolic tendon at the anchorage with a special load cell. For TB3, this load cell was not available.

Table 1: Prestressing forces and material properties

	TB1	TB2	TB3
External Prestr. [kN] ([kip])	0	270 (60.7)	450 (101.2)
$\sigma_{c,ext}$ [MPa] ([ksi])	0	1.5 (0.22)	2.5 (0.36)
Internal Prestr. [kN] ([kip])	430 (96.7)	430 (96.7)	430 (96.7)
$\sigma_{c,int}$ [MPa] ([ksi])	2.0 (0.29)	2.0 (0.29)	2.0 (0.29)
Friction coefficient μ [-]	0.206	0.195	---
$\varepsilon_{cc} + \varepsilon_{cs}$ [‰]	0.11	0.18	0.25
E_{cm} [MPa] ([ksi])	25810 (3743)	25140 (3646)	24460 (3548)
$f_{\mathrm{c,cyl}}$ [MPa] ([ksi])	36.9 (5.35)	38.6 (5.60)	39.6 (5.74)
$f_{\mathrm{ct,split}}$ [MPa] ([ksi])	2.94 (0.43)	3.09 (0.45)	2.92 (0.42)
$f_{\mathrm{ct,axial}}$ [MPa] ([ksi])	2.71 (0.39)	3.34 (0.48)	3.14 (0.46)

The values are in good compliance with the manufacturer's data of μ = 0.21. All test beams were tested 14 days after concreting and seven days after prestressing. Creep and shrinkage strains ε_{cc} and ε_{cs} were measured in the top flange in the midspan of the beam by mechanical extensometers. The concrete was designed as C30/37 concrete with a maximum aggregate size of 8 mm (0.31"). The modulus of elasticity E_{cm} and the concrete compressive strength $f_{c,cyl}$ were measured on three concrete cylinders (d = 150 mm (5.9"), h = 300 mm (11.8")) on the day of testing (14 days after concreting). In addition, the tensile strength of the concrete f_{ct} was measured by five uniaxial tensile tests, as well as by three split cylinder tests.

The cross-section of the specimens is shown in Fig. 5. The area of the top flange with a width of 50 cm (19.7”.) and a height of 16 cm (6.3”) is considerably larger than that of the bottom flange, only 30 cm (11.8”) wide. This is representative of existing prestressed box girders, in which the deck slab is larger than the bridge’s bottom slab. The beams had a flexural reinforcement of 8Ø12 (0.47”) in the top flange and 5Ø12 in the bottom flange, as shown. The bondless external tendons were positioned in the center line of the cross-section. The anchorage was located at the ends of the beam.

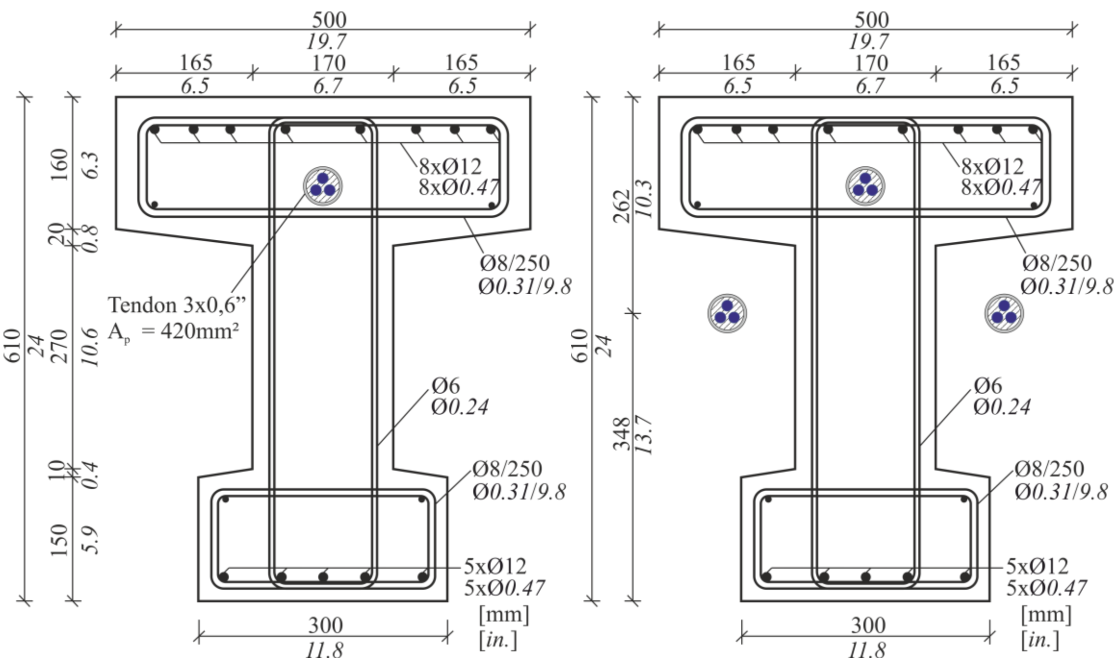

Fig. 5 *left*: Cross-section without external tendons
right: Cross-section with external tendons

TEST RESULTS

The final crack pattern of TB1 (no external prestressing) after both tests is shown in Fig. 6. The cracks that developed in the first part of the test are shown in black, whereas the cracks that occurred in the second part of the test after strengthening the beam are shown in blue. The first flexural cracks appeared above the mid support and beneath the load points at a load of about 190 kN (42.7 kip). The flexural cracks had almost reached the top flange in the span and the bottom flange above the support when the first shear cracks appeared at a load of 280 kN (62.9 kip). The stiffness of the beam was reduced instantly at this point, which can also be seen in the load deflection curves. At a load of 400 kN (89.9 kip), the shear cracks had already reached the compression zone at the load point on the side of the beam with a low amount of shear reinforcement. At this point, the test was stopped since the beam might have collapsed at any time, and the failed side was strengthened using tie rod, as shown. The second test was conducted on the same day, resulting in the final crack pattern. The maximum loads that were reached were 401 kN (90.1 kip) during the first test and 539 kN (121.2 kip) during the second test.

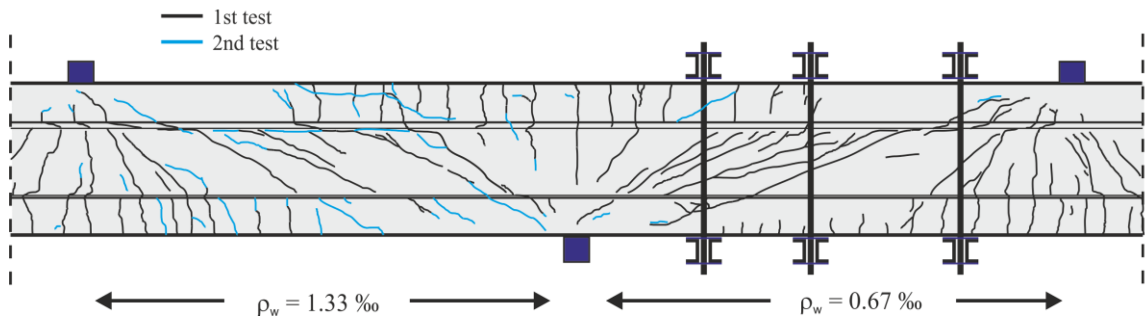

Fig. 6 Final crack pattern of TB1

The crack pattern of TB2 is shown in Fig. 6. Since additional external prestressing was applied to this beam, not as many flexural and shear cracks developed compared to TB1. The first flexural and shear cracks appeared simultaneously at a load of 314 kN (70.6 kip). The maximum loads were 435 kN (97.8 kip) and 483 kN (108.6 kip) for the first and second tests, respectively. This beam failed at a smaller shear force during the second test than TB1 because a large crack along the connection of the top flange and the web occurred at an early stage of the test, shown as AB in Fig. 7.

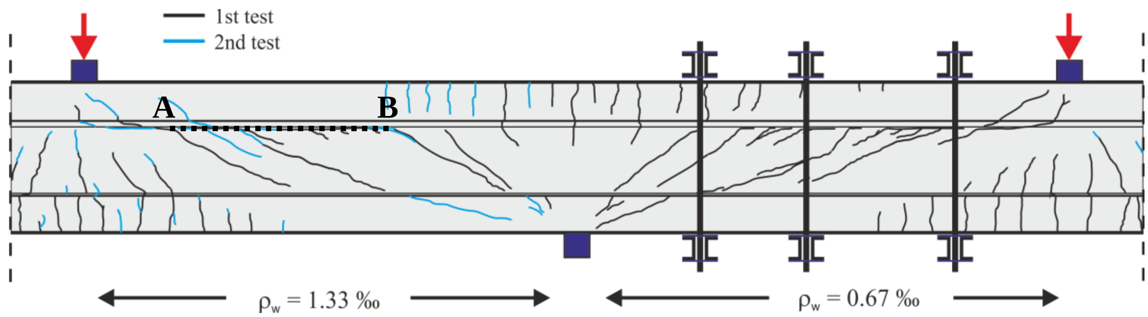

Fig. 7 Final crack pattern of TB2

The crack pattern of TB3 is shown in Fig. 8. The first flexural and shear cracks appeared at a load of 327 kN (74 kip). This beam had the least number of cracks and the smallest crack widths due to the high degree of external prestressing. The maximum loads were 447 kN (101 kip) and 525 kN (118 kip).

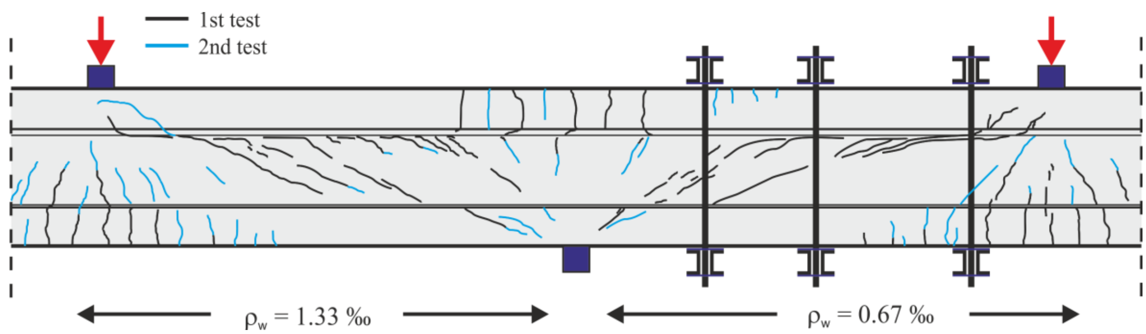

Fig. 8 Final crack pattern of TB3

The load-deflection curves of the test specimens are shown in Fig. 9. The beams with external prestressing (TB2 and TB3) resist higher shear forces at lower deflections. In particular, the external prestressing markedly increases the initial shear cracking load. As a consequence, the crack widths were considerably smaller with external prestressing, e.g. the average crack widths of TB2 with ρ_w = 0.067% were 20%-30% smaller than those for TB1.

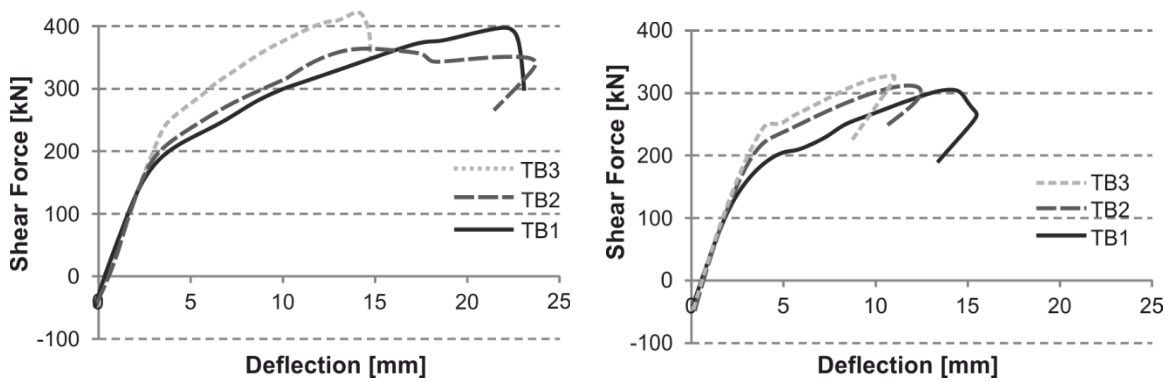

Fig. 9 *left*: load deflection curves for ρ_w = 0.133 %
right: load deflection curves for ρ_w = 0.067 %

The initial shear crack loads V_{crack} and the ultimate shear loads V_{ult} of the three test beams are summarized in Table 2. While initial shear crack loads increase by up to 44 % due to external prestressing, the ultimate loads only increase by 4 % and 7 %, respectively (Fig. 10, left). Although there is only a small amount of shear reinforcement in the test beams, the test loads could be increased considerably after the initial appearance of shear cracks, which is reflected in the ratio of ultimate shear loads V_{ult} and initial shear crack loads V_{crack} (Fig. 10, right). However, the ratio of V_{ult} and V_{crack} also decreases with additional external prestressing, which indicates that the degree of additional external prestressing should be limited for small amounts of shear reinforcement.

Table 2: Prestressing forces and material properties

	TB1		TB2		TB3	
ρ_w [%]	0.067	0.133	0.067	0.133	0.067	0.133
V_{crack} [kN]	170 (38 kip)	175 (39 kip)	210 (47 kip)	210 (47 kip)	245 (55 kip)	245 (55 kip)
V_{ult} [kN]	314 (71 kip)	403 (91 kip)	328 (74 kip)	366 (82 kip)	337 (76 kip)	418 (94 kip)

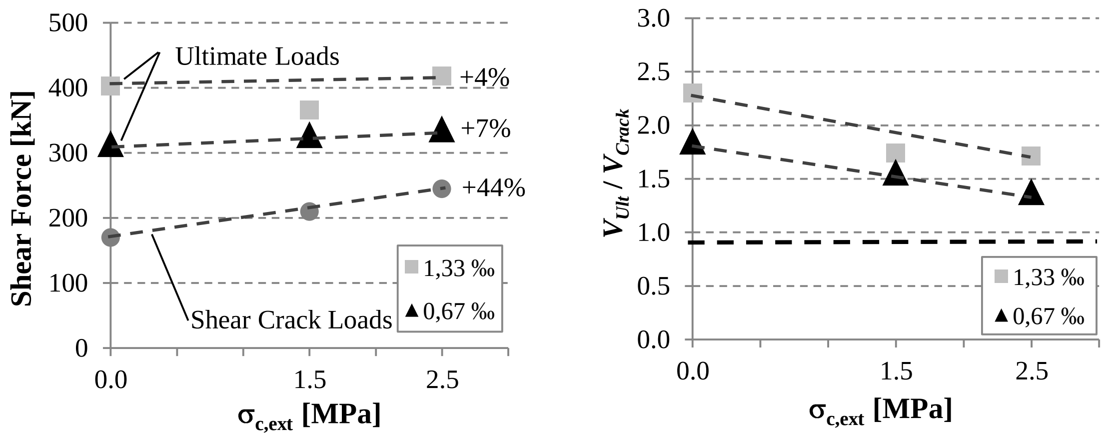

Fig. 10 *left*: Initial shear crack loads and ultimate loads;
right: Ratio of ultimate loads and shear crack loads

CALCULATED SHEAR CAPACITY

The shear capacity of the test beams was calculated according to different approaches using the measured concrete properties (mean values) and prestressing forces (Table 3). The shear capacity was calculated at a distance of 0.5 m (19.7") from the support. The shear capacity according to the German bridge design code DIN-FB 102 was calculated according to Eq. (1) (V_{MC90}), Eq. (2) (V_{TC}) and Eq. (3) (V_{TRUSS}). The shear capacity according to the approach by Goertz was calculated by Eq. (6) (V_{GOERTZ}). Additionally, the shear capacity was calculated according the Modified Compression Field Theory (MCFT)[15]. The so-called "Level III approximation" of the Model Code 2010[16] (V_{MC2010}) distinguishes between the truss and concrete contributions to the shear capacity of prestressed concrete beams and is based on the Simplified MCFT[17]. In this procedure, (which is almost identical to the general shear design procedure (section 5.8.3.4.2) of the AASHTO Bridge Design Specifications) the shear capacity must be calculated by iteration, since the strain of the cross-section due to loading is considered. The program Response2000 was used to calculate the shear capacity of the specimens according to the MCFT (V_{MCFT})[18].

Table 3: Experimental and calculated shear capacity according to different approaches

	TB1		TB2		TB3	
ρ_w [%]	0.067	0.133	0.067	0.133	0.067	0.133
V_{exp} [kN] ([kip])	319 (72)	409 (92)	333 (75)	372 (84)	342 (77)	423 (95)
V_{MC90} [kN] ([kip])	105 (24)	105 (24)	112 (25)	112 (25)	117 (26)	117 (26)
V_{TC} [kN] ([kip])	249 (56)	249 (56)	291 (65)	293 (66)	318 (71)	320 (72)
V_{TRUSS} [kN] ([kip])	105 (24)	153 (34)	105 (24)	154 (35)	105 (24)	155 (35)
V_{GOERTZ} [kN] ([kip])	251 (56)	277 (62)	265 (60)	299 (67)	263 (59)	299 (67)

V_{MC2010} [kN] ([kip])	133 (30)	207 (47)	162 (36)	248 (56)	189 (42)	285 (64)
V_{MCFT} [kN] ([kip])	335 (75)	335 (75)	351 (79)	351 (79)	386 (87)	386 (87)

The ratio of the experimental shear capacity V_{exp} and the calculated shear capacity V_{calc} according to the different approaches is illustrated in Fig. 11. The approach by the German Bridge Code seems to be conservative in the cases of Eq. (1) and Eq. (3). On the other hand, the approach of the main tensile criterion is very close to the ultimate loads of the test beams. Since this approach is supposed to predict the initial shear crack load, it seems that the shear capacity is overestimated by this approach. It was revealed that this is mainly due to the fact that the residual stresses by internal prestressing are neglected. If the residual stresses are taken into account, the main tensile criterion is able to predict the initial shear crack loads very precisely. The approach is still on the safe side since the loads could be increased for all test beams after the appearance of shear cracks because of the existing shear reinforcement. However, if more external prestressing were applied, the approach by the main tensile criterion might be unsafe, which is why the amount of external prestress should be limited. The approach by Goertz is in good agreement with the ultimate loads of the test beams because all major influences on the shear capacity of prestressed concrete beams are taken into account. The Level III approximation by the Model Code 2010 also yields better results than the truss model and the model from MC90 in the German Bridge Code. The shear capacity that was calculated by Response2000 is closest to the ultimate loads of the test beams, but it also overestimates the shear capacity of some beams.

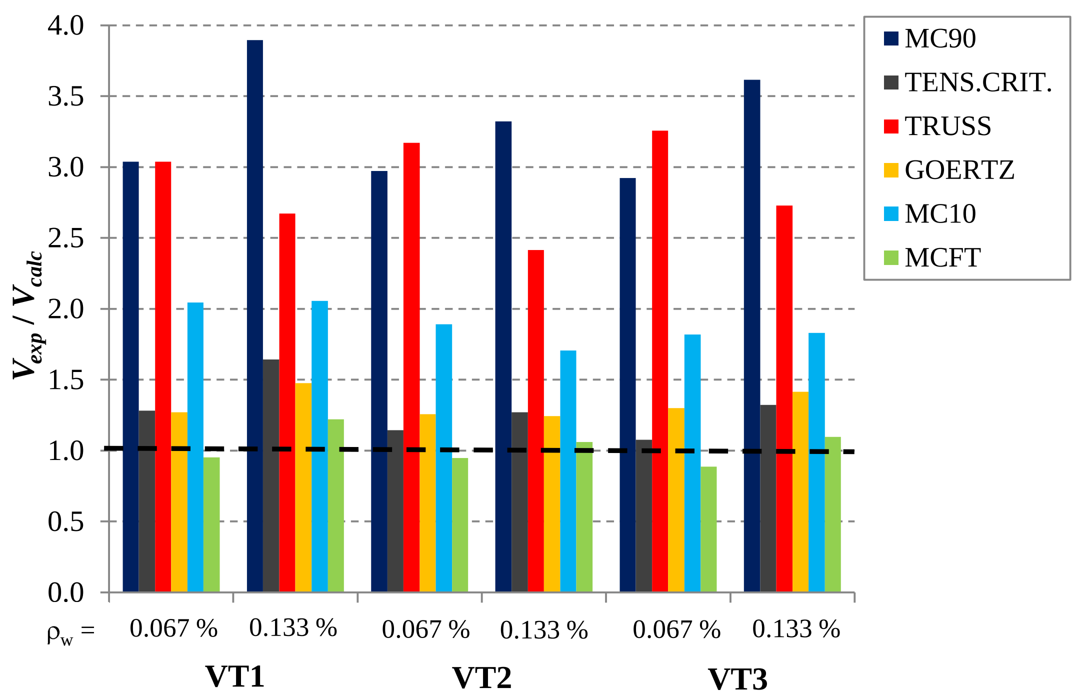

Fig. 11 Ratio of experimental and calculated shear capacity

FINITE ELEMENT PARAMETRICAL STUDIES

In order to verify some of the approaches further, additional parametrical studies by Finite Element Analysis were performed. The nonlinear finite element calculations were carried out based on the experimental investigations with the program Abaqus FEA. Results from previous projects have shown that the material behavior of concrete can be represented by the Concrete Damaged Plasticity Model, which is available in Abaqus[19,20]. The stirrups, the longitudinal reinforcement and the internal tendon were modeled using truss elements and plastic stress-strain relationships for steel, including softening. The elements have been embedded into to the concrete assuming full bond between the concrete and steel (Fig. 12, left). The forces of the external tendons were simulated by the application of pressure on the end plate of the beam, since there was no bond between the tendons and the concrete. The concrete was modeled using solid elements with eight nodes and reduced integration, using a fine mesh at the mid support with an edge length of 15 mm (0.59") to accurately capture the shear cracking. The rest of the beam was modeled using elements with a size of 50 mm (1.97"). The different areas were connected using a tie-constraint (Fig. 12, right). The number of elements in the model was reduced by using symmetry conditions in the model. Due to the highly non-linear problem, an explicit solution technique was used. The results of the simulations of the test beams have shown to be in good agreement with the test results.

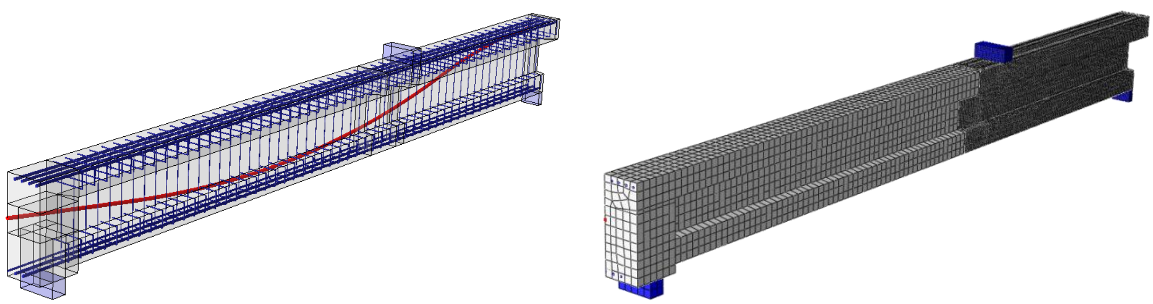

Fig. 12 *left*: steel reinforcement and internal tendon
right: mesh of the Finite Element model

For the parametrical studies four different types of beams were simulated:

- 23 beams with an I-profile and a parabolic tendon profile (I-PBL) (Fig. 13, (a)(d))
- 20 beams with an I-profile and a polygonal tendon profile (I-PLY) (Fig. 13, (a)(c))
- 23 beams with a T-profile and a parabolic tendon profile (T-PBL) (Fig. 13, (b)(d))
- 17 beams with an I-profile and a parabolic tendon profile. The concrete tensile strength and the facture energy were calculated according to an approach by Remmel[21] (I-PBL-RML)

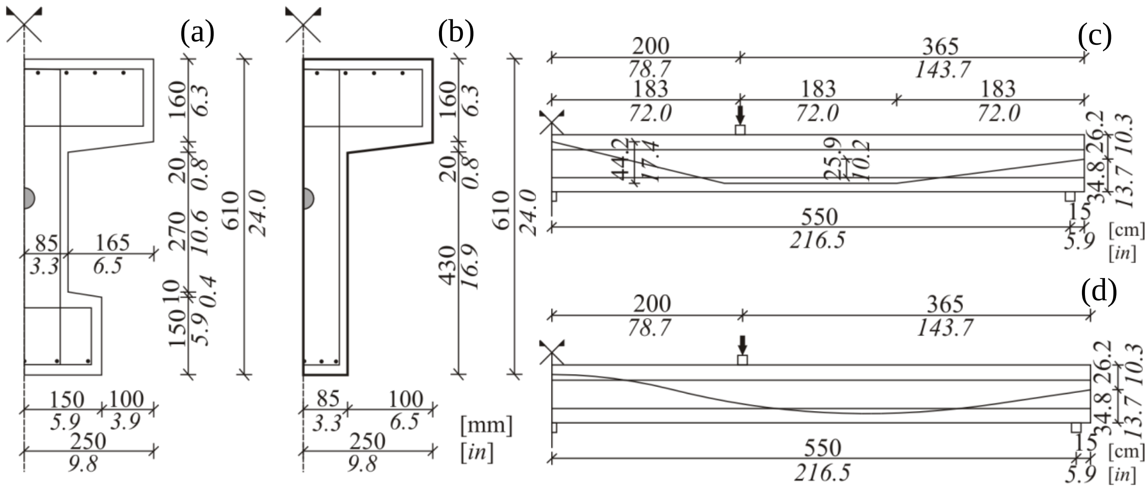

Fig. 13 *left*: Cross-section used in the parametrical study
right: Tendon profiles used in the parametrical study

Altogether, 83 numerical simulations were carried out. The internal and external degree of prestressing, the shear reinforcement ratio and the concrete compressive as well as the tensile strength were varied. The basic configuration of the parameters is summarized in Table 4.

Table 4: Prestressing forces and material properties

$\sigma_{c,int}$	$\sigma_{c,int}$	ρ_w	f_{ck}	f_{ctm}
[MPa]	[MPa]	[%]	[MPa]	[MPa]
2.0	1.5	0.15	35	$0.30 \cdot f_{ck}^{2/3}$

The results of the parametrical study are shown in Fig. 14.

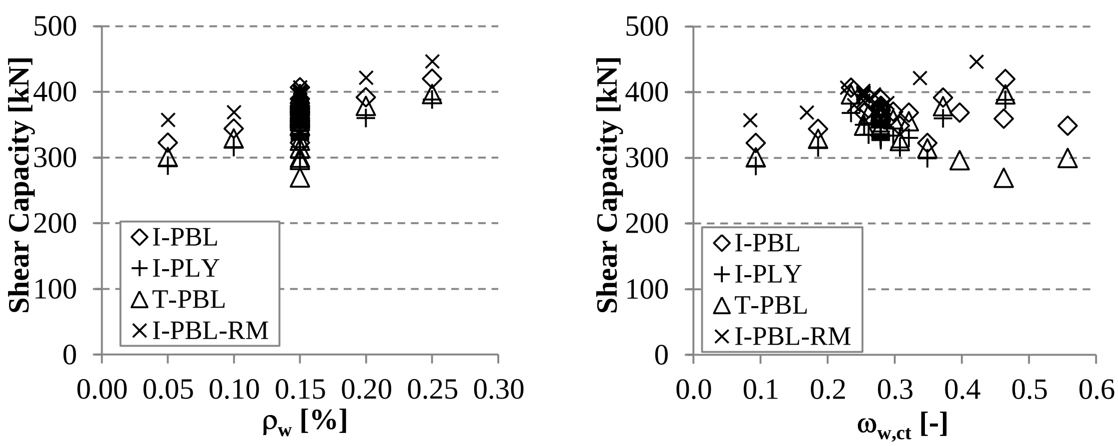

Fig. 14 *left*: Shear capacity V_{FEM} depending on the geometrical shear reinforcement ratio ρ_w
right: Shear capacity V_{FEM} depending on the mechanical shear reinforcement ratio $\omega_{w,ct}$

Naturally, the shear reinforcement ratio was the governing influence on the shear capacity. For reasons of readability, the results are also shown depending on the mechanical reinforcement ratio $\omega_{w,ct}$ (Fig. 14, left). The shear capacity of the Finite Element models was compared to the calculated shear capacity of the approach by the German Bridge Code according to Eq. (1) (V_{MC90}), and Eq. (3) (V_{TRUSS}) (Fig. 15).

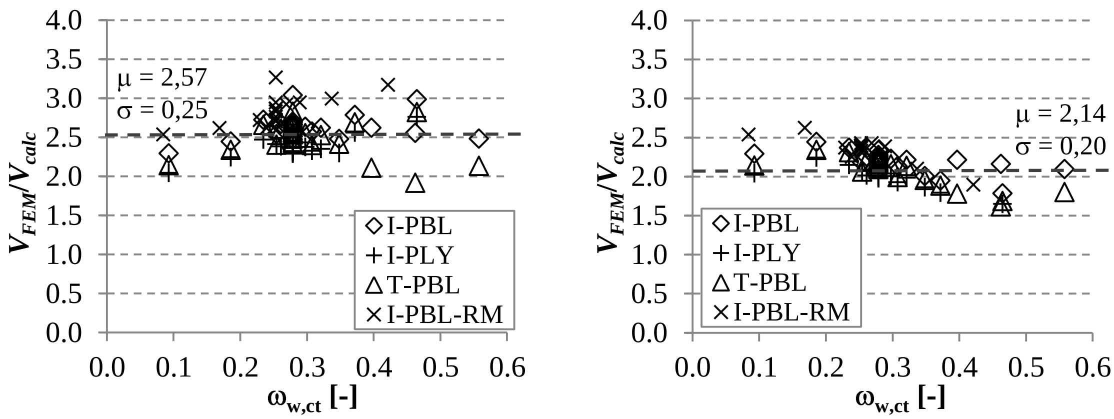

Fig. 15 *left*: Ratio of V_{FEM} and V_{calc} according to Eq. (1)
right: Ratio of V_{FEM} and V_{calc} according to Eq. (3)

The mean value of the shear capacity according the FEA and MC90 amounts to 2.57 with a standard deviation of 0.25 (Fig 15, left), whereas the mean value of FEA and the truss model is slightly better with a mean value of 2.14 and a standard deviation of 0.20 (Fig 15, right). Both models are conservative in predicting the ultimate loads of prestressed concrete continuous beams. The shear capacity of the FE models was also calculated using the approach by Goertz. The predicted loads are in good agreement with the ultimate loads of the FEA with a mean value of 1.22 and a standard deviation of 0.09 (Fig. 16, left). The ratio of FEA and calculated loads is also shown depending on the degree of external prestressing *m* (Eq.(11)) (Fig. 16, right). As shown, the influence of the external prestressing is considered appropriately by the approach by Goertz.

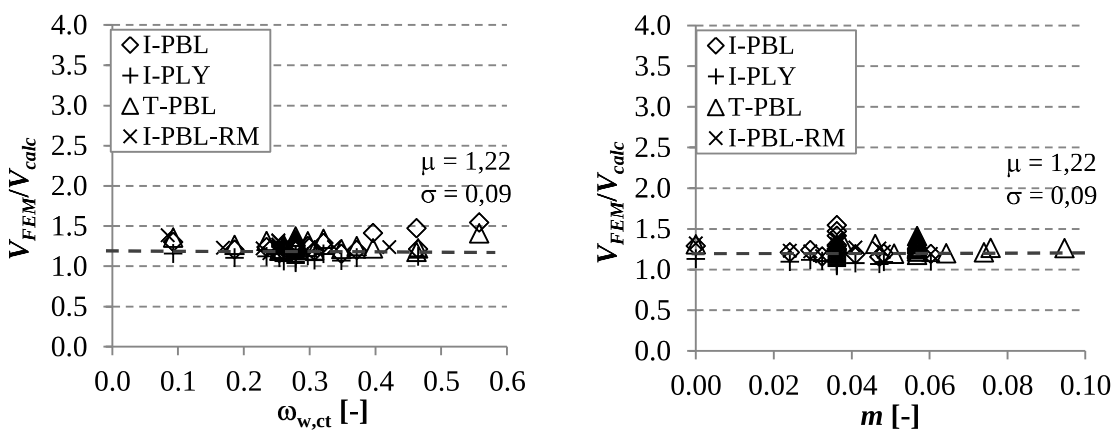

Fig. 16 *left*: Ratio of V_{FEM} and V_{calc} depending on $\omega_{w,ct}$
right: Ratio of V_{FEM} and V_{calc} according depending on *m*

CONCLUSIONS AND FUTURE WORK

Six tests on three prestressed two-span beams with different shear reinforcement ratios and different degrees of external prestressing have been performed. The ultimate shear capacity of the specimens was compared to the calculated shear capacity according to the German bridge design code DIN-FB 102, an approach by Goertz, and the Modified Compression Field Theory. The test results indicate that the approach according to the Model Code 90 and the truss model with crack friction underestimate the shear capacity of existing bridges. However, the shear check based on the main tensile criterion is in good agreement with the test results, as well as the approach by Goertz. The Level III approximation of the Model Code 2010, which is based on the Simplified Modified Compression Field Theory, underestimates the shear capacity of the test beams by a factor ranging from 1.7 to 2.1. On the other hand, the shear capacity according to the MCFT calculated by the program Response2000 predicts the shear capacity very precisely but overestimates the shear capacity in some cases by a factor of up to 1.1.

In general, the ultimate shear capacity was only increased slightly by external prestressing, but the initial shear crack loads increased by up to 44 %. This is especially beneficial if the shear check is performed with the main tensile criterion. In this regard, the application of additional external tendons can be a very effective measure to strengthen existing bridge structures. However, the degree of external prestressing should be limited to avoid immediate failure after the appearance of shear cracks. The tests also indicated that a small amount of shear reinforcement is sufficient to avoid immediate shear failure. Thus, additional rules for bridges without the required minimum shear reinforcement could help to extend their lifespan.

Additional parametrical studies with the Finite Element program Abaqus have shown that the approach by Goertz might by suitable for predicting the actual ultimate shear loads of existing bridges. In 83 different numerical simulations, the approach by Goertz has shown a very good agreement with the shear capacity predicted by FEA, with a mean value of V_{FEM} and V_{calc} of 1.22. Safety factors still need to be derived for this model in order to make it available for the redesign of bridges. Therefore, more tests on prestressed continuous concrete beams will be required in the future.

ACKNOWLEDGEMENTS

This publication is partially based on research findings of project FE-No. 15.0498/2010 on behalf of the Federal Ministry of Transport, Building and Urban Development (BMVBS) represented by the German Federal Highway Research Institute (BASt). The responsibility for the content remains with the authors. We acknowledge the funding and the discussions with the project committee.

REFERENCES

1. DIN 1072, German Design Code “Road bridges – Actions on bridges“, 1953.
2. Kaschner R., “Auswirkungen des Schwerlastverkehrs auf die Brücken der Bundesfernstraßen“, Iss. B68, Federal Highway Research Institute of Germany (BASt), July 2009

3. Ickert L., “Abschätzung der langfristigen Entwicklung des Güterverkehrs in Deutschland bis 2050“, Final Report for the Federal Ministry of Transport, Building and Urban Development of Germany, Basel 2007
4. DIN 4227, German Design Code “Prestressed concrete - Guidelines for design and construction“, 1953.
5. BMV-Richtlinie, German Design Guideline: “Additional provisions to DIN 4227 for prestressed concrete bridges“, 1969.
6. DIN Fachbericht 102, German Design Code “Concrete Bridges”, 2009.
7. Reineck K.-H., “Hintergründe zur Querkraftbemessung in DIN 1045-1 für Bauteile aus Konstruktionsbeton mit Querkraftbewehrung“, Bauingenieur 76, pp. 168-179, 2001.
8. CEN EN 1992-2 Eurocode 2, Design of concrete structures - Part 2: Concrete bridges – Design and detailing rules, Beuth Verlag GmbH, Germany, 2010.
9. DIN Fachbericht 101, German Design Code “Actions on Bridges”, 2009.
10. Hegger J., Goertz S., “Querkraftmodell für Bauteile aus Normalbeton und Hochleistungsbeton“, Beton- und Stahlbetonbau 101, Heft 9, pp. 695 – 705, 2006.
11. CEB-FIB Model Code 1990. Design Code. Bulletin d’Information No.213/214, Lausanne, 1991
12. Federal Ministry of Transport, Building and Urban Development, “Guidelines for Survey and Redesign of Bridges”, 2011.
13. Zink, M., “Zum Biegeschubversagen schlanker Bauteile aus Hochleistungsbeton mit und ohne Vorspannung.“ Doctoral thesis, University of Leipzig, 1999
14. HEGGER J., SHERIF A., GOERTZ S., “Investigation of Pre- and Postcracking Shear Behaviour of Prestressed Concrete Beams Using Innovative Measuring Techniques“, ACI Structural Journal, Vol. 100, No. 2, pp. 183 – 192, 2004.
15. Vecchio, F.J., Collins, M.P. “Modified Compression Field Theory for Reinforced Concrete Elements Subjected to Shear.” ACI Structural Journal, Vol. 83, No. 2, Mar.-Apr. 1986, pp. 219-231.
16. CEB-FIB Model Code 2010. Design Code Final Draft. Lausanne, 2011
17. Bentz, E.C., Vecchio, F.J., and Collins M.P., “Simplified Modified Compression Field Theory for Calculating Shear Strength of Reinforced Concrete Elements”, ACI Structural Journal,Vol. 103, July-Aug. 2006, pp. 614-624
18. Bentz, E.; Collins, M.P., “Response 2000 User Manual”, Version 1.1, September 2001
19. Lee J., Fenves G. L., “Plastic-Damage Model for Cyclic Loading of Concrete Structures“, Journal of Engineering Mechanics 124, No. 8, pp. 892–900, 1998.
20. Hegger J., Roggendorf T., Teworte F., “FE analyses of shear-loaded hollow-core slabs on different supports“, Magazine of concrete research, Vol. 62, No. 8, pp. 531-541, Thomas Telford, London, 2010.
21. Remmel, G., “Zum Zug- und Schubtragverhalten von Bauteilen aus hochfestem Beton“, German Committee for Structural Concrete, Issue 444, Berlin 1994